

Landauer's formula breakdown for radiative heat transfer and nonequilibrium Casimir forcesAdrián E. Rubio López,^{1,2,*} Pablo M. Poggi,³ Fernando C. Lombardo,³ and Vincenzo Giannini^{4,5}¹*Institute for Quantum Optics and Quantum Information of the Austrian Academy of Sciences, Technikerstrasse 21a, Innsbruck 6020, Austria*²*Institute for Theoretical Physics, University of Innsbruck, A-6020 Innsbruck, Austria*³*Departamento de Física Juan José Giambiagi, FCEyN UBA and IFIBA CONICET-UBA, Facultad de Ciencias Exactas y Naturales, Ciudad Universitaria, Pabellón I, 1428 Buenos Aires, Argentina*⁴*Department of Physics, Condensed Matter Theory, Imperial College London, London SW7 2AZ, United Kingdom*⁵*Instituto de Estructura de la Materia, IEM-CSIC, E-28006 Madrid, Spain*

(Received 28 September 2017; published 30 April 2018)

In this work, we analyze the incidence of the plates' thickness on the Casimir force and radiative heat transfer for a configuration of parallel plates in a nonequilibrium scenario, relating to Lifshitz's and Landauer's formulas. From a first-principles canonical quantization scheme for the study of the matter-field interaction, we give closed-form expressions for the nonequilibrium Casimir force and the heat transfer between plates of thicknesses d_L, d_R . We distinguish three different contributions to the Casimir force and the heat transfer in the general nonequilibrium situation: two associated with each of the plates and one to the initial state of the field. We analyze the dependence of the Casimir force and heat transfer with the plate thickness (setting $d_L = d_R \equiv d$), showing the scale at which each magnitude converges to the value of infinite thickness ($d \rightarrow +\infty$) and how to correctly reproduce the nonequilibrium Lifshitz's formula. For the heat transfer, we show that Landauer's formula does not apply to every case (where the three contributions are present), but it is correct for some specific situations. We also analyze the interplay of the different contributions for realistic experimental and nanotechnological conditions, showing the impact of the thickness in the measurements. For small thicknesses (compared to the separation distance), the plates act to decrease the background blackbody flux, while for large thicknesses the heat is given by the baths' contribution only. The combination of these behaviors allows for the possibility, on one hand, of having a tunable minimum in the heat transfer that is experimentally attainable and observable for metals and, on the other hand, of having vanishing heat flux in the gap when those difference are of opposite signs (thermal shielding). These features turns out to be relevant for nanotechnological applications.

DOI: [10.1103/PhysRevA.97.042508](https://doi.org/10.1103/PhysRevA.97.042508)**I. INTRODUCTION**

One of the most fundamental aspects of every physical theory describing quantum phenomena is dispersion, which unavoidably emerges in every formalism considered. This means that, at the quantum level, we always deal with dynamics that include background fluctuations, which enforces the employment of statistical quantities to describe the reality of nature.

Within this context, fluctuation features are found for every state of the system under study, even for the state of lowest energy. This state is usually called the “ground state” although in contexts involving the notion of particles it is also referred to as “vacuum state,” since it commonly corresponds to the state with zero number of particles or, in other words, without real particles. However, the statistical aspects allow for the concept of virtual particles, characterized by a ephemeral existence and then being part of fluctuational deviations of the particle number with respect to the number of real particles. Nevertheless, although these virtual particles seem to have no physical reality, the fluctuational deviations are precisely responsible of purely quantum phenomena that can be experimentally measured and

present no classical equivalent. That is how the quantum nature of vacuum takes part in the description of different physical situations (see Refs. [1,2]).

Within the context of quantum field theory (QFT), dispersion phenomena includes van der Waals–Casimir forces and heat transfer between micro- and macroscopic bodies, including micro and nanoelectromechanical systems (MEMS and NEMS; see Ref. [3]). Thus, the possibility of having completely quantum effects appearing at macroscales is a reality and studying them is of relevant interest from theoretical, experimental, and technological points of view (see Ref. [4]).

In the case of the van der Waals–Casimir force, there is a vast number of remarkable works analyzing different aspects related to multiple configurations, geometries (see, for example, Refs. [5–10]), and materials in different contexts (see Refs. [11–15], to mention a few). Moreover, there are also works studying thermodynamic aspects of the Casimir force involving dissipative materials (see Refs. [16–20]).

The previous research includes equilibrium and nonequilibrium situations. It should be noted that in the context of the dispersion phenomena addressed in this work (static Casimir forces and steady heat flux), “nonequilibrium” stands for steady situations (with time-independent quantities) that cannot be described as a thermodynamic equilibrium scenario between the parts of the total system considered.

*arubio@df.uba.ar

In the Casimir framework, it must be mentioned first that the pioneering work of Lifshitz (see Ref. [21]) was the first to shed light on the theoretical framework which allows us to include dissipative materials in the calculation of Casimir forces. In that work, he developed the basis of fluctuational quantum electrodynamics (FQED) by combining the electrodynamics in real media with the quantum fluctuation-dissipation theorem applied to the current sources at zero temperature. This demonstrates the fact that the Casimir force, existing even at zero temperature, is a macroscopic effect of quantum origin. The configuration that he analyzed was conformed by two parallel plates of infinite thickness (or half-spaces) separated by a vacuum gap. Although his result was valid for zero temperature, the finite-temperature generalization for half-spaces did not take long to be achieved also by Lifshitz and other author, but this time from a fully QFT approach (see Ref. [22]). The expression found for the force gives what it is now commonly referred as “Lifshitz formula.” In that work, the expression was given in the Matsubara representation. Nevertheless, the formula can be also written as an integral whose integrand is a product of two factors, one containing the information of the materials in the reflection coefficients of each half-space and another one including the temperature as the only parameter. Moreover, it was shown that in thermal equilibrium the expression for the Casimir force between finite-width plates results with the same form of the Lifshitz formula but the reflection coefficients are the ones for plates of finite thickness. Throughout this work, we will use “thickness” and “width” indistinctly for referring to the length of the parallel plates in the normal direction to its surfaces. Clearly, Lifshitz’s formula is reobtained from this result by taking the infinite-thickness limit for the plates, which is guaranteed by the fact that the finite-width reflection coefficients reduce to the ones for half-spaces (see Ref. [14] for a review on this).

It should be noted that, throughout Casimir physics, a crucial point is always to handle and subtract infinities that arise unavoidably in QFTs. In other words, for obtaining finite results, a regularization procedure has to be implemented. There are different methods for handling divergences depending on the situation analyzed. Beyond them, for parallel plates made of dissipative materials, no infrared divergences occur and the ultraviolet divergences are prevented by the natural cutoff provided by the dissipation in the material (see, for example, Ref. [23]), which takes into account the fact that the materials are transparent for high frequencies (for the case without dissipation, a cutoff function has to be introduced by hand to obtain a finite result). However, the result is infinite due to the inherent zero-point fluctuations. These divergences are contained in the mentioned factor associated to the materials in the integral form for the force. For two finite-width plates in thermal equilibrium, there are two methods for eliminating these divergences. One is the “Casimir prescription” (see Ref. [1]), consisting in calculating the energy contained in the gap between the plates and subtracting it with the energy contained in the same region and in the same situation (thermal equilibrium) for the case of free space, i.e., in absence of the plates. This method also applies for half-spaces. The other method is based on subtracting the radiation pressure at each side of one of the (finite-width) plates, which corresponds to the net force over the given plate (see Ref. [24], for example). Both

methods gives the mentioned finite-width formula at thermal equilibrium. Moreover, it is worth noting that both regularization procedures takes into account the specific scenario of thermal equilibrium in order to only affect the factor associated to the materials in a correct way.

On the other hand, for nonequilibrium scenarios, one can find research addressing configurations involving point dipoles, spheres, and half-spaces (see Refs. [19,25–30] and literature cited therein) based fundamentally in the FQED approach. A full QFT approach to nonequilibrium scenarios was recently developed in Ref. [31] and then successfully implemented to derive the half-spaces’ result obtained from FQED (see Ref. [32]). Also in these situations, regularization procedures are required. In FQED formalisms, this step is typically accomplished by discarding the bulk part of the Green’s tensor, which ensures that all the terms independent of the relative positions of the material bodies are effectively discarded. Thus, this can be seen as a third method that applies for very general situations, but within the context of a FQED approach (see also Refs. [33,34]).

To the best of our knowledge, there are no previous works dedicated to investigating whether the two methods described above for the study of finite-width plates in equilibrium can be implemented in situations out of equilibrium and how to do it in a conceptually clear approach. Moreover, the nonequilibrium version of the Lifshitz formula was obtained but not deduced from the finite-width case within the context of a full QFT approach. One recent work going in this direction is Ref. [24], where a canonical quantization formalism is developed to obtain the force between finite-width plates in a nonequilibrium scenario characterized by thermal and squeezed states but not addressing the previous question. Within this framework, the Casimir force is given by two types of contributions, one associated to the radiation generated by the plates and another one associated with the initial state of the field.

Now, we consider this approach to give a clear answer to this issue as part of the results of the present work. By considering an initial state for the field that gives a temperature for modes impinging the plates configuration from the left and another one to the modes impinging from the right, we show how in a nonequilibrium scenario the connection between the finite-width result and the nonequilibrium Lifshitz formula is achieved. This shows how to adapt the Casimir prescription for these situations, while the method based on the pressures subtraction leads to an incorrect result.

On the other hand, for the case of heat transfer, the phenomenon admits classical or quantum descriptions depending on the particular scenario. In the farfield, there are plenty of works describing the heat transfer in terms of classical frameworks based on electrodynamics combined with thermodynamics results (see Ref. [35]). The heat transfer between bodies at different temperatures is given by Stefan’s law of heat exchange (see also Refs. [36,37]), which is basically the difference between the blackbody radiation emitted by each body, only considering the statistical properties of propagating modes of the electromagnetic (EM) field. Additionally, when the macroscopic bodies have a particular shape, one can develop a theory implementing this law but weighted with the geometrical properties of the given configuration. This approach basically takes into account how much radiation emitted

from one body impinges the other. Within this framework, the radiation is treated in a thermodynamical way, without giving a specific description as EM waves.

As the typical distances involved in the situation addressed get shorter, far-field treatment is no longer valid and the wave nature of the EM field begins to become crucial. Propagating modes lead the heat exchange, but diffraction and interference-like phenomena could have an impact on some configurations. Moreover, in the near-field regime, the evanescent modes start to contribute, becoming a channel of heat transfer that cannot be neglected and which, in fact, could be the most important contribution in some situations. Then, a wave description of the EM radiation is mandatory. Moreover, when considering dissipative materials from first-principles models, low temperatures or entirely quantum objects (as magnetic moments of spin), the need of a quantum theory becomes relevant. Some aspects can be described in a semiclassical way, through a stochastic electrodynamic theory, but replacing the classical fluctuation-dissipation theorem by its quantum version, as it happens for FQED (see Refs. [1,34]). However, the development of a purely quantum approach enriches our understanding from a conceptual point of view and allows the study of regimes beyond the classical (see, for example, Refs. [38–40]).

The analog to Lifshitz's work for Casimir forces but in heat transfer is Ref. [41]. There, the authors developed a general EM theory and deduced the heat exchange between two half-spaces at different temperature. The approach includes propagating and evanescent modes' contributions and includes a quantum fluctuation-dissipation relation for the sources of current. The result obtained for the heat transfer has the form of Landauer's formula, where the heat is expressed as an integral over the frequencies with its integrand given by a product of two factors, one given by the difference of the boson occupation numbers of the radiations emitted by each body and another one including the geometrical and material properties of the bodies. This formula also predicts the enhancement of heat transfer in the near-field regime due to the growing of the evanescent modes' contribution. However, although it is widely used for different scenarios and configurations (see also Refs. [42,43]), another of the main achievements of the present work is to show that this formula is not valid in general for a finite-width plate configuration. Moreover, we show in which cases a Landauer's formula is obtained, gaining intuition about the physical properties of the different contributions that appear. Within the same scenario considered for the calculations regarding the force, we show that for the heat flux between the plates, Landauer's formula is not obtained for finite thickness, even if the initial state of the field is taken as the vacuum state (zero temperature). This is conceptually different from what it is analyzed in Refs. [42,43]. We consider that this understanding is crucial for the correct design of experiments at the micro- and nanoscale and also for the development and improvements of novel nanotechnological devices as MEMS and NEMS and, moreover, involving typical metals (see Ref. [12]).

All these features are studied and complemented with numerical calculations, exploiting some interesting phenomena that are expected with the physical intuition obtained.

In order to focus the main text of this work and the calculations on the mentioned results and the numerical

calculations, we have taken the formal results of Ref. [24] as a starting point and left some specific calculations and deductions to appendixes at the end of the paper. The paper is organized as follows: In the next section, we summarize the model, the field equation, and the steady solution for the field operator obtained in Ref. [24]. In Sec. III, we summarize the separation in contributions of the expectation value of the energy-momentum tensor, calculating general forms for arbitrary bodies but assuming thermal states for each bath and introducing an intrinsic nonequilibrium initial state for the field (the properties of this particular initial state for the field are also described in Appendix A). Then, we use these features to obtain the Casimir force and the heat flux between two plates of different thickness and materials (in Appendix B there are formulas complementing the obtained result). In Sec. IV, we study different aspects of the general formulas, showing that they reproduce all the previous (and well-known) results as particular cases, including Lifshitz's and Landauer's formulas. In Appendix C, there are some complementary calculations to this section. Section V is devoted to the numerical analysis for the case of identical plates (same material and thickness), showing the scale of convergence to the infinite-thickness expressions (given by Lifshitz's and Landauer's formulas) and the possibility of tuning the heat flux between the plates even to zero. Finally, Sec. VI summarizes our findings.

For simplicity, we have set $\hbar = k_B = c = 1$.

II. MODEL, TIME EVOLUTION, AND STEADY STATE

One way to address the matter-field interaction at a quantum level is to give a first-principles microscopic model for describing the quantum field in interaction with quantum degrees of freedom at each point of space (representing matter). In order to include effects of dissipation and noise in the description, we will use the theory of open quantum systems and treat the full field dynamics, having in mind the paradigmatic example of the quantum Brownian motion (QBM) [2].

In the present work, we consider the same model as the one employed in Ref. [24], that consists of a system composed of two parts: a massless scalar field and a dielectric material which, in turn, are described by their internal degrees of freedom (a set of harmonic oscillators); see Fig. 1.

Both subsystems conform a composite system which, in each point of space, is coupled to a second set of harmonic oscillators that plays the role of an external environment or thermal bath. For simplicity, we will work in 1 + 1 dimensions. In our toy model, the massless field represents the electromagnetic field, and the first set of harmonic oscillators directly coupled to the scalar field represents the polarizable volume elements of the material. In this model, the field and the volume elements of the material couples through a current-type one (mimicking the typical interaction term between the electromagnetic field and matter). The coupling constant for this interaction is the electric charge e . We will also assume that there is no direct coupling between the field and the thermal bath. Thus, the Lagrangian density is considered as

$$\begin{aligned} \mathcal{L} &= \mathcal{L}_\phi + \mathcal{L}_S + \mathcal{L}_{\phi-S} + \mathcal{L}_B + \mathcal{L}_{S-B} \\ &= \frac{1}{2} \partial_\mu \phi \partial^\mu \phi + 4\pi\eta \left[\frac{1}{2} m \dot{r}_x^2(t) - \frac{1}{2} m \omega_0^2 r_x^2(t) \right] \end{aligned}$$

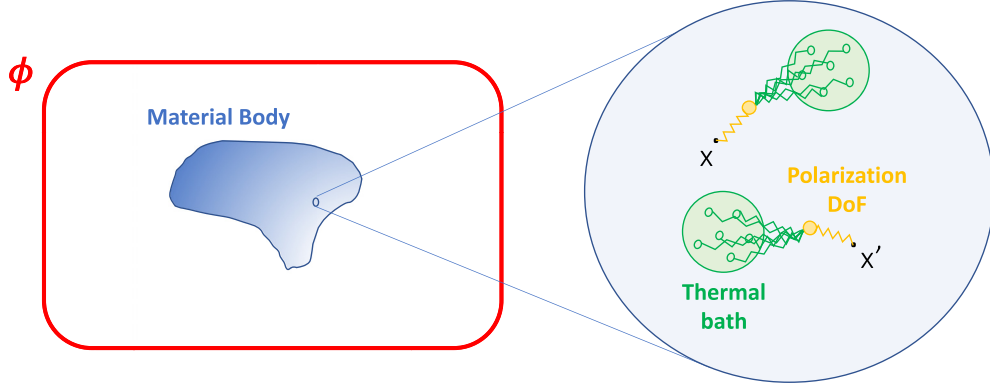


FIG. 1. Scheme of the composite system considered for the interaction field matter, expressed in the different terms of the Lagrangian in Eq. (1). It consists of two parts: the field ϕ and the material body. At the same time, each point of the material body is given by a polarization degree of freedom coupled to its own thermal bath (a set of harmonic oscillators).

$$\begin{aligned}
 & + 4\pi\eta e\phi(x,t)\dot{r}_x(t) \\
 & + 4\pi\eta \sum_n \left[\frac{1}{2}m_n\dot{q}_{n,x}^2(t) - \frac{1}{2}m_n\omega_n^2q_{n,x}^2(t) \right] \\
 & - 4\pi\eta \sum_n \lambda_n q_{n,x}(t)r_x(t), \quad (1)
 \end{aligned}$$

where the different terms on the right-hand side correspond to the different parts of the total composite system and its interactions. The first term corresponds to the Lagrangian of the massless scalar field. The second one, containing brackets, accounts for the polarization degrees of freedom of each volume element of the material, described as harmonic oscillators. The third contribution is the current-type interaction between the field and the degrees of freedom of the material. The fourth, also containing brackets, corresponds to the set of harmonic oscillators conforming the thermal bath. The last term is the (linear) interaction of the bath's oscillators with its respective volume element degree of freedom.

We have denoted the fact that r and q_n have a dependence on position with a label identifying the point of space at which they are located (but it is important to stress that this label is not a dynamical variable, as it happens for the scalar field). It is clear that each atom interacts with a thermal bath placed at the same position. We have denoted by η the density of the degrees of freedom of the volume elements. The constants λ_n are the coupling constants between the volume elements and the bath oscillators. It is implicitly understood that Eq. (1) represents the Lagrangian density inside the material, while outside the Lagrangian is given by the one of a free field.

The quantization of the theory is straightforward. It should be noted that the full Hilbert space \mathcal{H} of the model is not only the field Hilbert space \mathcal{H}_ϕ (as it is considered in others works where the field is the only relevant degree of freedom) but also includes the Hilbert spaces of the volume elements' degrees of freedom \mathcal{H}_A and the bath oscillators \mathcal{H}_B , in such a way that $\mathcal{H} = \mathcal{H}_\phi \otimes \mathcal{H}_A \otimes \mathcal{H}_B$. We will assume, as frequently done in the context of QBM, that for $t < t_0$ the three parts of the systems are uncorrelated and not interacting. Interactions are turned on at $t = t_0$. Therefore, the initial conditions for the operators $\hat{\phi}$, \hat{r} must be given in terms of operators acting in each part of the Hilbert space. The interactions will make that

initial operators to become operators over the whole space \mathcal{H} . The initial density matrix of the total system is of the form

$$\hat{\rho}(t_0) = \hat{\rho}_{IC}(t_0) \otimes \hat{\rho}_A(t_0) \otimes \hat{\rho}_B. \quad (2)$$

In principle, each part of the whole system can be in any initial state. Then, following Ref. [24] we can straightforwardly write the Heisenberg equations of motion and solve those related to the material's degrees of freedom and introduce it in the corresponding field equation to obtain an effective equation for the full dynamics of the field operator:

$$\begin{aligned}
 \square\hat{\phi} + \frac{\partial^2}{\partial t^2} \left[\int_{t_0}^t d\tau \chi_x(t-\tau)\hat{\phi}(x,\tau) \right] \\
 = 4\pi\eta eC(x) \left[\ddot{G}_2(t-t_0)\hat{r}_x(t_0) + \dot{G}_2(t-t_0)\frac{\hat{p}_x(t_0)}{m} \right. \\
 \left. + \int_{t_0}^t d\tau \dot{G}_2(t-\tau)\frac{\hat{F}_x(\tau-t_0)}{m} \right], \quad (3)
 \end{aligned}$$

where $\chi_x(t) = \omega_{p1}^2 G_{2,x}(t)C(x)$ is the susceptibility function with $\omega_{p1}^2 = \frac{4\pi\eta e^2}{m}$ being the plasma frequency and $G_{2,x}$ being the retarded Green's function associated to the QBM equation at the point x , $\hat{r}_x(t_0)$ and $\hat{p}_x(t_0)$ are the position and momentum operator of the volume element degrees of freedom of the material, and \hat{F}_x is the stochastic force operator generated by the bath at x which acts over the corresponding volume element. As can be seen in Ref. [24], this operator is a generalization of the stochastic force operator found in the quantum Brownian theory (within an open quantum system framework; see Ref. [2]) and it is characterized by its correlations given by a fluctuation-dissipation relation:

$$\begin{aligned}
 \left\{ \left\{ \hat{F}_{x'}^\infty(\omega'), \hat{F}_{x''}^\infty(\omega'') \right\} \right\}_B = (2\pi)^2 \delta(x' - x'') \frac{J(\omega')}{2\eta} \\
 \times \coth\left(\frac{\beta_{B,x'}\omega'}{2}\right) \delta(\omega' + \omega''), \quad (4)
 \end{aligned}$$

where $\beta_{B,x'}$ corresponds to the inverse temperature of the thermal bath located at x' (see Fig. 1 and Ref. [24] for more details).

It is worth noting that we have included a spatial label denoting the straightforward generalization to inhomogeneous

media, where each point of the material can have different properties. Beyond this dependence, the boundaries of the material bodies enter through the spatial material distribution function C , which is zero in free space points. The regions filled (and the contours) with real material are defined by this function. This is clearly essential for the determination of the field's boundary conditions.

Equation (3) can be solved in terms of the retarded Green's function $\mathfrak{G}_{\text{Ret}}$ after initial conditions for the field operator are given. In Ref. [24], this procedure has been done by giving free field initial conditions for the field operator, which are expressed in terms of the annihilation and creation operators $[\hat{a}_k(t_0), \hat{a}_k^\dagger(t_0)]$ of the free field. Therefore, at the initial time t_0 , the field is only an operator acting on \mathcal{H}_ϕ but switching on the interactions causes the field operator to become an operator which acts on the full Hilbert space \mathcal{H} during the time evolution:

$$\begin{aligned} \hat{\phi}(x, t) = & \hat{\phi}_{\text{IC}}(x, t) \otimes \mathbb{I}_A \otimes \mathbb{I}_B + \mathbb{I}_\phi \otimes \hat{\phi}_A(x, t) \otimes \mathbb{I}_B \\ & + \mathbb{I}_\phi \otimes \mathbb{I}_A \otimes \hat{\phi}_B(x, t). \end{aligned} \quad (5)$$

However, as we are interested in the expressions for the heat transfer and the Casimir force in nonequilibrium but steady situations, we require the long-time limit ($t_0 \rightarrow -\infty$) of the total field operator. The full expressions for each part during the time evolution and also the deduction of its long-time expressions for the present model can be found in Ref. [24], and we obtain

$$\begin{aligned} \hat{\phi}(x, t) \longrightarrow \hat{\phi}^\infty(x, t) = & \hat{\phi}_{\text{IC}}^\infty(x, t) \otimes \mathbb{I}_A \otimes \mathbb{I}_B + \mathbb{I}_\phi \otimes \hat{\phi}_A^\infty \otimes \mathbb{I}_B \\ & + \mathbb{I}_\phi \otimes \mathbb{I}_A \otimes \hat{\phi}_B^\infty(x, t), \end{aligned} \quad (6)$$

with each long-time operator given by

$$\begin{aligned} \hat{\phi}_{\text{IC}}^{(+),\infty}(x, t) = & \int_{-\infty}^{+\infty} dk \left(\frac{1}{\omega k} \right)^{1/2} \hat{a}_k(-\infty) \{ e^{-ikt} \Theta(k) \Phi_{-ik}^>(x) \\ & + e^{ikt} \Theta(-k) [\Phi_{-ik}^<(x)]^* \}, \end{aligned} \quad (7)$$

$$\hat{\phi}_A^{(+),\infty} = -\frac{1}{2} \int dx' \frac{4\pi\eta e C(x')}{\sqrt{2m\omega_0}} \hat{b}_{0,x'}(-\infty), \quad (8)$$

$$\begin{aligned} \hat{\phi}_B^\infty(x, t) = & \int dx' \frac{4\pi\eta e C(x')}{m} \int_{-\infty}^{+\infty} \frac{d\omega}{2\pi} e^{-i\omega t} i\omega \bar{G}_2(\omega) \\ & \times \bar{\mathfrak{G}}_{\text{Ret}}(x, x', \omega) \hat{F}_{x'}^\infty(\omega), \end{aligned} \quad (9)$$

where Φ^\lessgtr are the homogeneous solutions associated to the homogeneous field equation and satisfy only the boundary condition on each limit of the variable value's interval, $\hat{b}_{0,x'}(-\infty)$ is the annihilation operator of the volume element degree of freedom, and the overlines denote Fourier transforms.

III. FORCE AND RADIATIVE HEAT EXCHANGE AT THE STEADY STATE

With the field operator at the steady state, we can evaluate both the Casimir force and the heat transfer between two plates in an unified way by calculating the expectation values of the energy-momentum tensor operator. The quantum version of the energy-momentum tensor is obtained by symmetrizing the classical expression after promoting the field to a quantum

operator, giving

$$\begin{aligned} \hat{T}_{\mu\nu}(x_1^\sigma, t_0) \equiv & (\delta_\mu^\gamma \delta_\nu^\alpha - \frac{1}{2} \eta_{\mu\nu} \eta^{\gamma\alpha}) \frac{1}{2} [\partial_\gamma \hat{\phi}(x_1^\sigma) \partial_\alpha \hat{\phi}(x_1^\sigma) \\ & + \partial_\alpha \hat{\phi}(x_1^\sigma) \partial_\gamma \hat{\phi}(x_1^\sigma)]. \end{aligned} \quad (10)$$

As the field operator in the steady state is given by Eq. (6), by noting that the contribution associated to the volume elements is independent of time and space, we have that for the derivatives holds $\partial_\mu \hat{\phi}^\infty = \partial_\mu \hat{\phi}_{\text{IC}}^\infty \otimes \mathbb{I}_A \otimes \mathbb{I}_B + \mathbb{I}_\phi \otimes \mathbb{I}_A \otimes \partial_\mu \hat{\phi}_B^\infty$. Therefore, the volume elements has no contribution to the expectations values of the energy-momentum tensor. Moreover, as shown in Ref. [24], the expectation values of the annihilation and creation operators are zero for thermal states and we are considering thermal states for the baths. This turns out to be enough to prove that the expectation value of the energy-momentum tensor splits into two contributions, one associated to the initial conditions of the field and the other one associated to the baths:

$$\langle \hat{T}_{\mu\nu}(x_1^\sigma) \rangle = \langle \hat{T}_{\mu\nu}^{\text{IC},\infty}(x_1^\sigma) \rangle_\phi + \langle \hat{T}_{\mu\nu}^{\text{B},\infty}(x_1^\sigma) \rangle_{\text{B}}, \quad (11)$$

where $\langle \dots \rangle_{\phi, \text{B}} = \text{Tr}_{\phi, \text{B}}(\rho_{\text{IC}, \text{B}} \dots)$, denoting that each trace is taken in the corresponding part of the total Hilbert space.

Nevertheless, while for the baths we assume thermal states, for the field we will consider an intrinsic nonequilibrium state that takes into account the possibility for the initial free field to be in a state with net radiation going from left to right. Although the configuration is surrounded by free space, it is of phenomenological interest to consider a scenario where the configuration of plates is in contact with a general reservoir (i.e., the plates are inside an oven) with its left and right walls located at $x = -\infty$ and $x = +\infty$ respectively and having each one at different (inverse) temperature $\beta_{\phi, \text{L}}$ and $\beta_{\phi, \text{R}}$. Initially, before the appearance of the plates, having this situation clearly generates an intrinsic flow of heat from the hottest wall to the coldest one. After the appearance of the plates, during the transient stage, this flow is modified by the presence of the plates (as it happens in Ref. [24] for the field in an initial thermal state) until reaching the (steady) long-time regime.

Therefore, as the walls of the (hypothetical) oven are held at different temperatures, the crucial point here is that the modes representing traveling waves from left to right ($k > 0$) will radiate at the inverse temperature $\beta_{\phi, \text{L}}$, while the modes representing traveling waves from right to left ($k < 0$) will radiate at the inverse temperature $\beta_{\phi, \text{R}}$. Then, the intrinsic nonequilibrium state for the field will be defined by the expectation values:

$$\begin{aligned} \langle \hat{a}_k(-\infty) \hat{a}_{k'}(-\infty) \rangle_\phi &= 0, \\ \langle \hat{a}_k^\dagger(-\infty) \hat{a}_{k'}(-\infty) \rangle_\phi &= [\Theta(k) N_{\phi, \text{L}}(\omega_k) + \Theta(-k) N_{\phi, \text{R}}(\omega_k)] \\ &\quad \times \delta(k - k'), \end{aligned} \quad (12)$$

where the typical expectation values for a thermal state (see Ref. [24]) are simply recovered by setting $\beta_{\phi, \text{L}} = \beta_{\phi, \text{R}}$. More about the intrinsic nonequilibrium state is shown in Appendix A. In Fig. 2, a scheme of the configuration of plates within our formalism can be found.

Considering this, for a general configuration, both terms of the expectation value of the components of the energy-momentum tensor can be calculated by employing

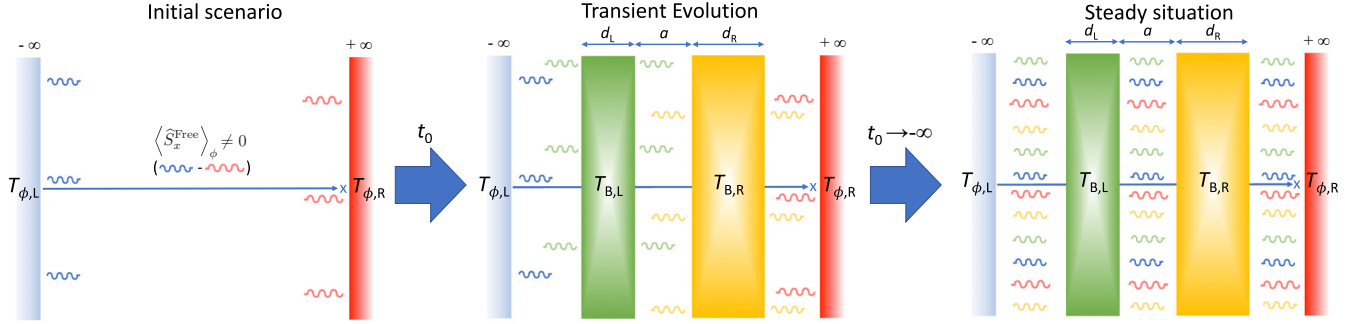


FIG. 2. Scheme of the configuration of plates within the canonical quantization formalism employed. The initial time corresponds to $t = t_0$ and the plates are not interacting with the scalar field. The field is free and it has a state of net heat flux different from zero. This information is encoded in the chosen “intrinsic nonequilibrium state” defined by Eq. (12) and commented in Appendix A. The amount of net heat flux is defined by the temperatures $T_{\phi,L,R}$, that can be interpreted as the temperatures of the walls of the hypothetical oven where the plates are placed. At $t = t_0$ the interaction of the field with the plates starts, having a transient stage that reaches a steady situation ($t_0 \rightarrow -\infty$). All the points of each plates are assumed to be at a given temperature $T_{B,L,R}$ (each body has a uniform temperature). In the steady situation, there is radiation emitted by the plates and by the walls of the hypothetical oven in all the regions and with all directions, due to the reflections in the bodies. In this situation, the Casimir force and the heat flux are evaluated.

the Green’s function and the homogeneous solutions for the given problem, obtaining the following expressions:

$$\begin{aligned} \langle \widehat{T}_{\mu\nu}^{\text{IC},\infty}(x_1^\sigma) \rangle_\phi &= \int_{-\infty}^{+\infty} dk \frac{1}{\omega_k} \left[\Theta(k) \coth\left(\frac{\beta_{\phi,L}\omega_k}{2}\right) + \Theta(-k) \coth\left(\frac{\beta_{\phi,R}\omega_k}{2}\right) \right] \text{Re}[(\delta_\mu^0(-i\omega_k)\Phi_k + \delta_\mu^1\Phi_k') \\ &\times [\delta_\nu^0 i\omega_k(\Phi_k)^* + \delta_\nu^1(\Phi_k')^*] - \frac{\eta_{\mu\nu}}{2}(\omega_k^2|\Phi_k|^2 - |\Phi_k'|^2)], \end{aligned} \quad (13)$$

$$\begin{aligned} \langle \widehat{T}_{\mu\nu}^{\text{B},\infty}(x) \rangle_{\text{B}} &= \int dx' C(x') \int_{-\infty}^{+\infty} d\omega \frac{\omega^2}{2} \text{Re}(n_{x'}) \text{Im}(n_{x'}) \coth\left(\frac{\beta_{\text{B},x'}\omega}{2}\right) \left([\delta_\mu^0(-i\omega) + \delta_\mu^1\partial_x] \overline{\mathfrak{G}}_{\text{Ret}}(x, x', \omega) [\delta_\nu^0 i\omega + \delta_\nu^1\partial_x] \mathfrak{G}_{\text{Ret}}^*(x, x', \omega) \right. \\ &\left. + [\delta_\mu^0(-i\omega) + \delta_\mu^1\partial_x] \mathfrak{G}_{\text{Ret}}^*(x, x', \omega) [\delta_\nu^0 i\omega + \delta_\nu^1\partial_x] \overline{\mathfrak{G}}_{\text{Ret}}(x, x', \omega) - \eta_{\mu\nu}[\omega^2|\overline{\mathfrak{G}}_{\text{Ret}}(x, x', \omega)|^2 - |\partial_x \overline{\mathfrak{G}}_{\text{Ret}}(x, x', \omega)|^2] \right), \end{aligned} \quad (14)$$

where in the initial conditions’ contribution we have used the notation that $\Phi_k(x) = \Phi_{-ik}^>(x)$ for $k > 0$ while $\Phi_k(x) = (\Phi_{-ik}^<(x))^*$ for $k < 0$, and $\omega_k = |k|$.

However, for a specific material configuration the homogeneous solutions Φ (from which the Green’s function can be constructed in a straightforward way) have to be calculated. If we consider a configuration of two plates of thickness $d_{L,R}$ respectively and different homogeneous materials separated by a distance a and surrounded by vacuum, those solutions Φ can be determined easily (see Ref. [24]). As we are considering a nonequilibrium situation, the Casimir force will be calculated from the expectation value of the xx component of the energy-momentum tensor, evaluated in the region between the plates and subtracting it with the same quantity in the absence of the plates’ configuration. This prescription is exactly the Casimir prescription for regularizing the expression of the force that here we apply for a nonequilibrium situation. It is worth noting that the method employing the radiation pressures at each sides of one of the plates (as is done for instance in Ref. [24] and references therein) is not applicable for this situation since it gives an incorrect regularization for the force and, moreover, different values of the force acting each plate. However, we can say that both approaches agree when the same state (thermal or not) is considered for each plate and for all the modes of the initial conditions’ contribution (as happens in Ref. [24]). Therefore, the Casimir force is given by

$$F_C = \langle \widehat{T}_{xx}^{\text{Free}} \rangle_\phi - \langle \widehat{T}_{xx}^{\infty} \rangle_{\text{Int}} = \langle \widehat{T}_{xx}^{\text{Free}} \rangle_\phi - \langle \widehat{T}_{xx}^{\text{IC},\infty} \rangle_\phi^{\text{Int}} - \langle \widehat{T}_{xx}^{\text{B},\infty} \rangle_{\text{B}}^{\text{Int}}, \quad (15)$$

where $\langle \widehat{T}_{xx}^{\text{Free}} \rangle_\phi$ is given by Eq. (A3). It is worth mentioning that the temperatures in the regularization term $\langle \widehat{T}_{xx}^{\text{Free}} \rangle_\phi$ will be taken as $\beta_{\phi,L,R}$ since it corresponds to a situation without plates and entirely defined by the walls of the (big) oven.

Therefore, each contribution is given by

$$\begin{aligned} \langle \widehat{T}_{xx}^{\text{IC},\infty} \rangle_\phi^{\text{Int}} [a, d_L, d_R, \beta_{\phi,L}, \beta_{\phi,R}] &= \int_0^{+\infty} dk k \left[\coth\left(\frac{\beta_{\phi,L}k}{2}\right) (|C_{-ik}^>|^2 + |D_{-ik}^>|^2) + \coth\left(\frac{\beta_{\phi,R}k}{2}\right) (|C_{-ik}^<|^2 + |D_{-ik}^<|^2) \right] \\ &= \int_0^{+\infty} dk k \frac{[\coth\left(\frac{\beta_{\phi,L}k}{2}\right) |t_L|^2 (1 + |r_R|^2) + \coth\left(\frac{\beta_{\phi,R}k}{2}\right) |t_R|^2 (1 + |r_L|^2)]}{|1 - r_L r_R e^{i2ka}|^2}, \end{aligned} \quad (16)$$

$$\begin{aligned}
 & \langle \widehat{T}_{xx}^{B,\infty} \rangle_B^{\text{Int}} [a, d_L, d_R, \beta_{B,L}, \beta_{B,R}] \\
 &= \int_0^{+\infty} d\omega \frac{\omega}{2} \left(\coth \left[\frac{\beta_{B,L}\omega}{2} \right] \text{Re}(n_L) \frac{(1 + |r_R|^2)}{|t_R|^2} \left\{ |E_{-i\omega}^<|^2 e^{-\omega \text{Im}(n_L)a} [1 - e^{-2\omega \text{Im}(n_L)d_L}] \right. \right. \\
 & \quad \left. \left. + |F_{-i\omega}^<|^2 e^{\omega \text{Im}(n_L)a} [e^{2\omega \text{Im}(n_L)d_L} - 1] + 2 \frac{\text{Im}(n_L)}{\text{Re}(n_L)} \text{Im}[E_{-i\omega}^{<*} F_{-i\omega}^< e^{-i\omega \text{Re}(n_L)a} (1 - e^{-i2\omega \text{Re}(n_L)d_L})] \right\} \right. \\
 & \quad \left. + \coth \left[\frac{\beta_{B,R}\omega}{2} \right] \text{Re}(n_R) \frac{(1 + |r_L|^2)}{|t_L|^2} \left\{ |E_{-i\omega}^>|^2 e^{-\omega \text{Im}(n_R)a} [1 - e^{-2\omega \text{Im}(n_R)d_R}] + |F_{-i\omega}^>|^2 e^{\omega \text{Im}(n_R)a} [e^{2\omega \text{Im}(n_R)d_R} - 1] \right. \right. \\
 & \quad \left. \left. + 2 \frac{\text{Im}(n_R)}{\text{Re}(n_R)} \text{Im}[E_{-i\omega}^{>*} F_{-i\omega}^> e^{-i\omega \text{Re}(n_R)a} (1 - e^{-i2\omega \text{Re}(n_R)d_R})] \right\} \right), \quad (17)
 \end{aligned}$$

and the coefficients for the plate configuration $C_{-ik}^{\leq}, D_{-ik}^{\leq}, E_{-ik}^{\leq}, F_{-ik}^{\leq}$ for each mirror $r_{L,R}, t_{L,R}$ and for an interface $r_{n_{L,R}}$ can be found in the Appendix B.

It is worth noting that each contribution results are symmetric under the interchange of the subscripts L and R, which means that the force has the same absolute value for both plates (with opposite signs on each one) and also that the inverted configuration of plates and oven walls provides the same forces.

In analogy, the heat between the plates is calculated as the expectation value of the Poynting vector in the region between the plates. In 1+1 dimensions, the Poynting vector has only one component corresponding to minus the x_0 component of the energy-momentum tensor. Then, the heat presents the same structure of contributions as the Casimir force:

$$Q_\infty \equiv \langle \widehat{S}_x^\infty \rangle = -\langle \widehat{T}_{x0}^\infty \rangle = Q_\infty^{\text{IC}}(a, d_L, d_R, \beta_{\phi,L}, \beta_{\phi,R}) + Q_\infty^{\text{B}}(a, d_L, d_R, \beta_{B,L}, \beta_{B,R}), \quad (18)$$

where each contribution is given by

$$\begin{aligned}
 Q_\infty^{\text{IC}}(a, d_L, d_R, \beta_{\phi,L}, \beta_{\phi,R}) &= \int_0^{+\infty} dk k \left[\coth \left(\frac{\beta_{\phi,L}k}{2} \right) (|C_{-ik}^>|^2 - |D_{-ik}^>|^2) - \coth \left(\frac{\beta_{\phi,R}k}{2} \right) (|C_{-ik}^<|^2 - |D_{-ik}^<|^2) \right] \\
 &= \int_0^{+\infty} dk k \frac{[\coth(\frac{\beta_{\phi,L}k}{2})|t_L|^2(1 - |r_R|^2) - \coth(\frac{\beta_{\phi,R}k}{2})|t_R|^2(1 - |r_L|^2)]}{|1 - r_L r_R e^{i2ka}|^2}, \quad (19) \\
 Q_\infty^{\text{B}}(a, d_L, d_R, \beta_{B,L}, \beta_{B,R}) &= \int_0^{+\infty} d\omega \frac{\omega}{8} \left(\coth \left[\frac{\beta_{B,L}\omega}{2} \right] \text{Re}(n_L) \frac{(1 - |r_R|^2)}{|t_R|^2} \left\{ |E_{-i\omega}^<|^2 e^{-\omega \text{Im}(n_L)a} [1 - e^{-2\omega \text{Im}(n_L)d_L}] \right. \right. \\
 & \quad \left. \left. + |F_{-i\omega}^<|^2 e^{\omega \text{Im}(n_L)a} [e^{2\omega \text{Im}(n_L)d_L} - 1] + 2 \frac{\text{Im}(n_L)}{\text{Re}(n_L)} \text{Im}[E_{-i\omega}^{<*} F_{-i\omega}^< e^{-i\omega \text{Re}(n_L)a} (1 - e^{-i2\omega \text{Re}(n_L)d_L})] \right\} \right. \\
 & \quad \left. - \coth \left[\frac{\beta_{B,R}\omega}{2} \right] \text{Re}(n_R) \frac{(1 - |r_L|^2)}{|t_L|^2} \left\{ |E_{-i\omega}^>|^2 e^{-\omega \text{Im}(n_R)a} [1 - e^{-2\omega \text{Im}(n_R)d_R}] \right. \right. \\
 & \quad \left. \left. + |F_{-i\omega}^>|^2 e^{\omega \text{Im}(n_R)a} [e^{2\omega \text{Im}(n_R)d_R} - 1] \right. \right. \\
 & \quad \left. \left. + 2 \frac{\text{Im}(n_R)}{\text{Re}(n_R)} \text{Im}[E_{-i\omega}^{>*} F_{-i\omega}^> e^{-i\omega \text{Re}(n_R)a} (1 - e^{-i2\omega \text{Re}(n_R)d_R})] \right\} \right). \quad (20)
 \end{aligned}$$

In this case (contrary to what happens to the force), the interchange of L and R is antisymmetric in any of the contributions, denoting the fact that if the configuration of plates and oven walls is reversed, the flux of heat goes in the opposite direction, as expected.

Equations (15)–(20) are the main results that we will analyze in the relevant (limit) cases in order to study the effect of thickness in the total expressions for both the force and heat in the nonequilibrium scenario.

Nevertheless, we get a simpler expression for the total heat by employing a relation between parts of the integrands regarding the materials that are based on the fact that in equilibrium ($\beta_{\phi,L} = \beta_{\phi,R} = \beta_{B,L} = \beta_{B,R} = \beta$) the total heat transfer is zero. In other words, as we have

$$Q_\infty(a, d_L, d_R, \beta, \beta, \beta) = Q_\infty^{\text{IC}}(a, d_L, d_R, \beta, \beta) + Q_\infty^{\text{B}}(a, d_L, d_R, \beta, \beta) \equiv 0, \quad (21)$$

this gives us a relation between the part of the integrands in Eqs. (19) and (20) involving the material properties since the thermal factors are the same for every term. Then, using this relation, we can write the total heat (in general) by mixing the contributions,

$$\begin{aligned}
 & Q_\infty(a, d_L, d_R, \beta_{\phi,L}, \beta_{\phi,R}, \beta_{B,L}, \beta_{B,R}) \\
 &= \int_0^{+\infty} dk 2k \frac{\{[N_{\phi,L}(k) - N_{B,R}(k)]|t_L|^2(1 - |r_R|^2) - [N_{\phi,R}(k) - N_{B,L}(k)]|t_R|^2(1 - |r_L|^2)\}}{|1 - r_L r_R e^{i2ka}|^2}
 \end{aligned}$$

$$\begin{aligned}
& + \int_0^{+\infty} dk \frac{k}{2} \frac{(1 - |r_R|^2)}{|1 - r_L r_R e^{i2ka}|^2} [N_{B,L}(k) - N_{B,R}(k)] \frac{(1 - |r_{n_L}|^2)}{|1 - r_{n_L}^2 e^{i2k n_L d_L}|^2} \left\{ (1 + |r_{n_L}|^2 e^{-2k \text{Im}(n_L) d_L}) (1 - e^{-2k \text{Im}(n_L) d_L}) \right. \\
& \left. + \frac{4 \text{Im}(n_L) e^{-2k \text{Im}(n_L) d_L}}{|n_L + 1|^2 (1 - |r_{n_L}|^2)} \text{Im}[r_{n_L} (1 - e^{i2k \text{Re}(n_L) d_L})] \right\}, \quad (22)
\end{aligned}$$

where we have used the fact that the factor containing the temperatures reads $\coth[\frac{\beta_{j,L}\omega}{2}] - \coth[\frac{\beta_{j,R}\omega}{2}] = 2[N_{j,L}(\omega) - N_{j,R}(\omega)]$, being $N_{j,L,R}$ the boson occupation numbers for each temperature.

Therefore, in general, the total heat flux does not have a Landauer's form, but each of the terms contributing does. As we have written the total heat flux, all the terms are expressed in terms of the differences between the occupation numbers of each part and the occupation number in the right plate. This can be changed by using the identity resulting from Eq. (21) in a different way, taking as reference another of the occupation numbers.

IV. IMPACT OF THICKNESS: ANALYTICAL RESULTS

Once we have obtained general expressions for both the Casimir force and the heat transfer between the plates of finite width, we can recover different well-known results as limiting cases and analyze particular features to gain understanding of the physics enclosed in the general formulas.

For the case of the Casimir force, part of the features were studied in Ref. [24] for the case when $\beta_{\phi,L} = \beta_{\phi,R} \equiv \beta_{\phi}$. Now, we will summarize the relevant findings of that work and give generalizations of them based on the introduction of the intrinsic nonequilibrium initial state for the field.

First, the result for materials without dissipation can be recovered since $\text{Im}(n_i) \equiv 0$, which immediately gives $\langle \widehat{T}_{xx}^{B,\infty} \rangle_{\text{NoDiss}}^{\text{Int}} \equiv 0$ and the Casimir force is only due to the initial conditions' contribution and the regularization term. Given the intrinsic nonequilibrium state, the Casimir force in this case is given directly by the subtraction of Eqs. (A3) and (16), but considering real refraction indexes.

Moreover, the Lifshitz formula for the Casimir force can also be deduced from our general expressions. However, there is a subtle point that must be considered. This is how to impose Lifshitz's scenario (consisting in two half-spaces at thermal equilibrium) in our expressions. On one hand, we have to take the infinite-thickness limit as $d_{L,R} \rightarrow +\infty$ and, on the other hand, we have to impose that all the temperatures are equal, $\beta_{B,L} = \beta_{B,R} = \beta_{\phi,L} = \beta_{\phi,R} \equiv \beta$. This last subtle point is crucial for deriving the correct expression for the force between half-spaces from the finite-thickness result, since for the latter situation, three contributions enter in the expression of the force: initial conditions, bath contributions, and the regularization term, each one with its own pair of temperatures. However, when taking $d_{L,R} \rightarrow +\infty$, the initial conditions' term vanishes ($\langle \widehat{T}_{xx}^{\text{IC},\infty} \rangle_{\phi}^{\text{Int}} \rightarrow 0$), while the other two do not. As shown in Ref. [24], for a half-space configuration, there will be no initial condition contribution at the steady state because there is no infinite-size empty regions anywhere. In this sense, the pressure calculated and also the regularization term will be both considered with $\beta_{B,L}$ and $\beta_{B,R}$. For this case, having the

same temperature for both half-spaces ($\beta_{B,L} = \beta_{B,R} \equiv \beta$) is enough to obtain the Lifshitz formula, regardless of the initial state of the field. However, from a conceptual point of view, if we want to obtain the Lifshitz formula as an infinite-thickness limit of the finite-width result, taking $d_{L,R} \rightarrow +\infty$ together with $\beta_{B,L} = \beta_{B,R} \equiv \beta$, it is not enough when $\beta_{\phi,L,R} \neq \beta$ in the regularization term. Clearly, by also putting $\beta_{\phi,L} = \beta_{\phi,R} \equiv \beta$, the total Casimir force takes the form of the Lifshitz formula.

Nonetheless, as we are introducing the intrinsic nonequilibrium initial state, we can go further and give also an expression for the nonequilibrium version of Lifshitz's formula, i.e., the force between two half-spaces when the temperatures are different from each other. To do this, we have to not only take the limit of infinite thickness ($d_{L,R} \rightarrow +\infty$) but also impose conditions over the temperatures $\beta_{\phi,L,R}, \beta_{B,L,R}$. From the analysis done for the equilibrium case, it is clear that in the nonequilibrium case the temperatures must be grouped in left and right, realizing the fact that each of the half-spaces is in local equilibrium. Therefore, we have to impose $\beta_{\phi,L} = \beta_{B,L} \equiv \beta_L$ and $\beta_{\phi,R} = \beta_{B,R} \equiv \beta_R$. As shown in Appendix C, the infinite-thickness limit of Eq. (17) is given by Eq. (C2) while Eq. (16) vanishes.

Then, by setting $\beta_{\phi,L} = \beta_{B,L} \equiv \beta_L$ and $\beta_{\phi,R} = \beta_{B,R} \equiv \beta_R$, the total Casimir force for the limit of infinite thickness ($d_{L,R} \rightarrow +\infty$) in a nonequilibrium scenario is

$$\begin{aligned}
& F_C[a, d_{L,R} \rightarrow +\infty, \beta_L, \beta_R, \beta_L, \beta_R] \\
& = \int_0^{+\infty} d\omega \omega \left[\coth\left(\frac{\beta_L \omega}{2}\right) \left(1 - \frac{[1 - |r_{n_L}|^2][1 + |r_{n_R}|^2]}{|1 - r_{n_L} r_{n_R} e^{i2\omega a}|^2}\right) \right. \\
& \left. + \coth\left(\frac{\beta_R \omega}{2}\right) \left(1 - \frac{[1 - |r_{n_R}|^2][1 + |r_{n_L}|^2]}{|1 - r_{n_L} r_{n_R} e^{i2\omega a}|^2}\right) \right], \quad (23)
\end{aligned}$$

which is the generalization of Lifshitz's formula for the case of nonequilibrium, from which the usual Lifshitz's formula is obtained by simply setting $\beta_L = \beta_R \equiv \beta$.

It is worth noting that the chosen prescription to obtain the Casimir force in this nonequilibrium situation gives the correct expression, while the approach in which the force is calculated from the difference of the radiation pressures at each side of a given plate gives an incorrect result in this scenario but a correct one in the equilibrium case.

On the other hand, for the heat transfer between the plates, similar analysis can be done, exposing different conceptual properties than for the force.

A first crucial difference is that this quantity needs no regularization term since it is, from the beginning, a subtraction of the radiations traveling in each directions. Moreover, as we showed in Eq. (21), the total heat flux, in equilibrium, vanishes. This is achieved since the contributions cancel between each other. Nevertheless, it should be noted that having $\beta_{\phi,L} = \beta_{\phi,R} = \beta_{\phi} \neq \beta_B = \beta_{B,L} = \beta_{B,R}$ does not give vanishing total

heat flux from the formula, which is also physically true since the scenario is an out-of-equilibrium one.

Regarding the contributions, it should be noted that the initial conditions' contribution Q_∞^{IC} basically measures the asymmetry between the blackbody radiations that reach the configuration from the left and the right with different temperatures. In other words, the heat transfer associated to the initial conditions' contribution gives the difference between the radiations coming from left and right after passing the plate corresponding to the side that they come from. It is the net difference between the blackbody radiations coming from the outside of the plates' configuration after

interacting with the plates. In fact, that contribution for $d_{L,R} = 0$ recovers exactly Stefan's law of blackbody heat exchange.

On the other hand, the heat transfer associated to the baths is the difference in the radiation generated by each plate that reaches the other one. In this case, for $d_{L,R} = 0$, the contribution automatically cancels. Moreover, as it is expected, the contribution also vanishes for dissipationless materials since $\text{Im}(n_i)$.

For the case of identical plates (unique material and same thickness), both contributions to the heat transfer between the plates take the form

$$Q_\infty^{\text{IC}}(a, d, d, \beta_{\phi,L}, \beta_{\phi,R})|^{1-\text{Mat}} = \int_0^{+\infty} dk k [N_{\phi,L}(k) - N_{\phi,R}(k)] \frac{|t|^2(1 - |r|^2)}{|1 - r^2 e^{i2ka}|^2}, \quad (24)$$

$$Q_\infty^{\text{B}}(a, d, d, \beta_{B,L}, \beta_{B,R})|^{1-\text{Mat}} = \int_0^{+\infty} d\omega \omega [N_{B,L}(\omega) - N_{B,R}(\omega)] \frac{|t|^2(1 - |r|^2)}{|1 - r^2 e^{i2ka}|^2} \frac{|n+1|^2}{8|n|^2} \{ \text{Re}(n)(e^{2\omega \text{Im}(n)d} - 1) + \text{Re}(n)|r_n|^2(1 - e^{-2\omega \text{Im}(n)d}) + 2\text{Im}(n)\text{Im}[r_n(1 - e^{i2\omega \text{Re}(n)d})] \}, \quad (25)$$

where both contributions have the form of a Landauer-like formula. Then, it can be easily checked now that, for the case of equal temperature on both sides for each contribution ($\beta_{j,L} = \beta_{j,R} = \beta_j$), the heat transfers automatically vanish. This leads to a subtle point, associated with the fact that for the situation of two identical plates (same width and material), we can have that both contributions vanish regardless if the temperatures of the contributions is the same. In other words, we can have that the total heat transfer vanishes although $\beta_\phi \neq \beta_B$. This particular feature of the heat shows the different natures of the contributions that enters the calculations in the decomposition of the field operator acting in the total Hilbert space as a sum of operators acting in each Hilbert subspaces associated to each part of the composite system [Eq. (6)]. Moreover, we can switch on one of the contributions independently whether the other one vanishes or not, allowing a separately study of each of the contributions. If we like to switch on the initial conditions' contribution, it is enough to set $\beta_{\phi,L} \neq \beta_{\phi,R}$ while $\beta_{L,B} = \beta_{R,B}$. If we like the contrary, it is enough to set $\beta_{\phi,L} = \beta_{\phi,R}$ while $\beta_{L,B} \neq \beta_{R,B}$.

Finally, we can say that for the case of identical plates, the total heat transfer Q_∞ can be given by a Landauer formula by setting $\beta_{\phi,L} = \beta_{L,B} = \beta_L \neq \beta_{\phi,R} = \beta_{R,B} = \beta_R$:

$$Q_\infty(a, d, d, \beta_L, \beta_R, \beta_L, \beta_R)|^{1-\text{Mat}} = \int_0^{+\infty} d\omega \omega [N_L(\omega) - N_R(\omega)] \frac{|t|^2(1 - |r|^2)}{|1 - r^2 e^{i2ka}|^2} \times \left(1 + \frac{|n+1|^2}{8|n|^2} \{ \text{Re}(n)(e^{2\omega \text{Im}(n)d} - 1) + \text{Re}(n)|r_n|^2(1 - e^{-2\omega \text{Im}(n)d}) + 2\text{Im}(n)\text{Im}[r_n(1 - e^{i2\omega \text{Re}(n)d})] \} \right). \quad (26)$$

The other case of interest also for the heat transfer is the infinite-thickness case ($d_{L,R} \rightarrow +\infty$). It is straightforward that when $d_{L,R} \rightarrow +\infty$, the initial conditions' contribution vanishes regardless of whether the material of both plates is the same; i.e., $Q_\infty^{\text{IC}}(a, d_{L,R} \rightarrow +\infty, \beta_{\phi,L}, \beta_{\phi,R}) \equiv 0$. Although a difference in the material of each plate is allowed, because the configuration is asymmetric, the infinite size of each plate cancels the contribution of the radiation impinging from outside the configuration, giving a zero initial condition contribution for the heat in contrast to what happen for the case of the force.

On the other hand, the baths' contribution takes the form

$$Q_\infty^{\text{B}}(a, d_{L,R} \rightarrow +\infty, \beta_{B,L}, \beta_{B,R}) = \int_0^{+\infty} d\omega \omega [N_{B,L}(\omega) - N_{B,R}(\omega)] \frac{[1 - |r_{n_L}|^2][1 - |r_{n_R}|^2]}{|1 - r_{n_L} r_{n_R} e^{i2\omega a}|^2}, \quad (27)$$

which is a Landauer-like formula, but different from the previous case of unique material. Again, given this formal

Landauer-like expression, if we take $\beta_{B,L} = \beta_{B,R} = \beta$, the contribution vanishes regardless of whether the material is the same.

Therefore, for the infinite-thickness case ($d \rightarrow +\infty$), we can say that the total heat transfer Q_∞ is also given by a Landauer formula, regardless of the temperature of the radiation outside the configuration, which in this case never reaches the gap between plates.

However, regardless of these cases, the general case does not correspond to Landauer's formula, as we commented at the end of the previous section. Moreover, even considering the same temperature for the traveling modes ($\beta_{\phi,L} = \beta_{\phi,R}$), the total heat flux cannot be written as Landauer's formula when the plates have finite width. Even when setting the temperature of the traveling modes equal to zero (and therefore, having $N_{\phi,j} \equiv 0$), the total heat flux is not given by Landauer's formula although it depends only on the baths' temperatures.

In conclusion, the total heat transfer Q_∞ is not always given by a Landauer-like formula. Moreover, it also presents different

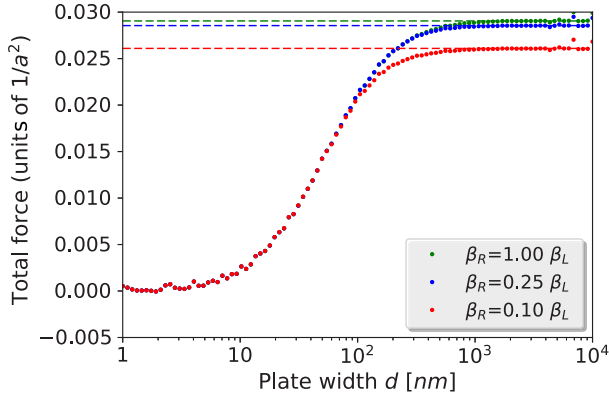


FIG. 3. Total Casimir force as a function of the width of the plates d for a left temperature $T_L = \frac{1}{\beta_L} = 300$ K and different right temperatures T_R . Equilibrium and nonequilibrium cases are considered. Parameters are $\gamma_{L,R} = 10^{-1}/a$, $\omega_{0,i} = 10/a$, $\omega_{pl,i} = 10/a$, and $a = 100$ nm.

limiting behaviors than for the force, enclosing different physical aspects. The general case of finite-width plates of different materials presents both contributions $[Q_{\infty}^{IC}(a, d_L, d_R, \beta_{\phi,L}, \beta_{\phi,R})$ and $Q_{\infty}^B(a, d_L, d_R, \beta_{B,L}, \beta_{B,R})]$ different from zero, positioning the nonequilibrium scenario ($\beta_{\phi,L} \neq \beta_{\phi,R} \neq \beta_{B,L} \neq \beta_{B,R}$) as very rich and highly nontrivial in the interplay with the thickness role. In the next section, we investigate some aspects that can be addressed by numerical analysis.

V. IMPACT OF THE THICKNESS: NUMERICAL RESULTS

Given the exact analysis done in the previous section, it is interesting to study numerically how the width of the plates combined with the nonequilibrium features included in the general result give interesting physical aspects and let us explore the impact of the thickness in dispersion phenomena.

In this sense, including the possibility of having different temperatures but the same finite width for both plates ($d_L = d_R \equiv d$), there are remarkable physical effects that can be interpreted within our theoretical framework.

A crucial question that initially drives this numerical analysis and that is also of experimental interest is the following: Given the formulas for finite-width plates, which is the thickness from which the value of the total force does not differ significantly from the value of infinite-width plates ($d \rightarrow +\infty$)? In other words, for which scale of thickness d is the value of the total force closer to the value for $d \rightarrow +\infty$? Moreover, from the measurement of the force, for which scale of d we can say that the plates act effectively as plates of infinite thickness? From which thickness can a plate of finite width be considered practically as an infinite-width plate?

On the other hand, some questions that appear related to this analysis are the following: Is this scale the same for equilibrium and nonequilibrium scenarios? It is also the same if the quantity considered is the heat transfer between the plates? Is it the same physics for the different contributions? Moreover, are there other remarkable physical effects that appear for different values of the thickness in nonequilibrium scenarios? Are these effects tunable in some way?

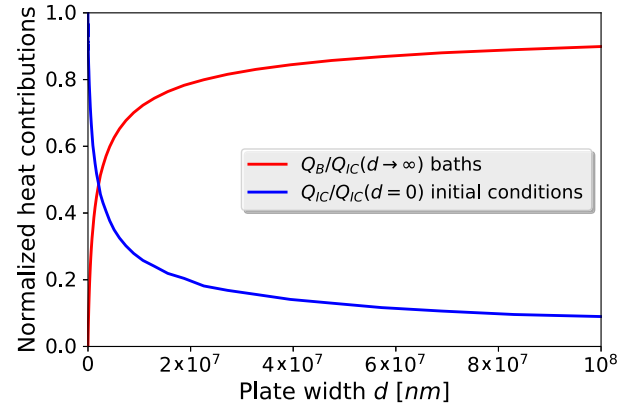


FIG. 4. Normalized contributions to the total heat as a function of the width of the plates for a right temperature $T_{\phi,R} = T_{B,R} = 300$ K and different left temperatures $T_{\phi,L} = T_{B,L}$. Note that the initial conditions' contribution is normalized with the value at $d = 0$ (which corresponds to Stefan's law), since the contributions goes to zero for $d \rightarrow +\infty$, while the baths' contribution is normalized in the opposite way given its behavior. Parameters are $\gamma_{L,R} = 10^{-1}/a$, $\omega_{0,i} = 10/a$, $\omega_{pl,i} = 10/a$, and $a = 100$ nm.

Figure 3 shows the behavior of the total Casimir force of Eq. (15) as a function of the thickness d for both equilibrium and nonequilibrium scenarios. The dashed lines correspond to the asymptotic values ($d \rightarrow +\infty$) of the total Casimir force given by Eq. (23). It can be observed that the scale of convergence with the thickness is of the order of the separation a between the plates.

Therefore, for a given separation of the plates, a plate can be considered of infinite width when the thickness is greater than the separation distance.

It is also worth noting that the force is maximized in the equilibrium case. Moreover, it decreases when there is more thermal difference between the plates, regardless of which plate is at higher temperature. This can be physically explained since in a nonequilibrium scenario, there is a momentum exchange taking place in the region between the plates that it is not present in the equilibrium case and tends to separate the plates. Therefore, the total force between the plates decreases in value, regardless of which plate is at a higher temperature.

If we now study what happens with the heat transfer between the plates, the situation changes. In Fig. 4, we observe both contributions to the total heat as a function of the plate width d .

It is clear that the convergence is achieved in a very different scale than for the force. In order to differ by less than 10% from its asymptotic value, the thickness of the plate has to be greater than 10^6 times the separation of the plates a . This means that the contributions to the heat transfer are more sensitive to the plates' width than the force in several orders of magnitude. Given the independence on the switching of each contribution, this scale could be measured by adjusting the physical parameters of the configuration (material properties and temperatures) in the appropriate way.

Moreover, it is worth noting that, on the one hand, for $d = 0$ (corresponding to the left side of the Fig. 4) we have $Q_{\infty}^B \equiv 0$ while $Q_{\infty}^{IC} \neq 0$, giving the value corresponding to the heat transfer between distant objects at given temperatures

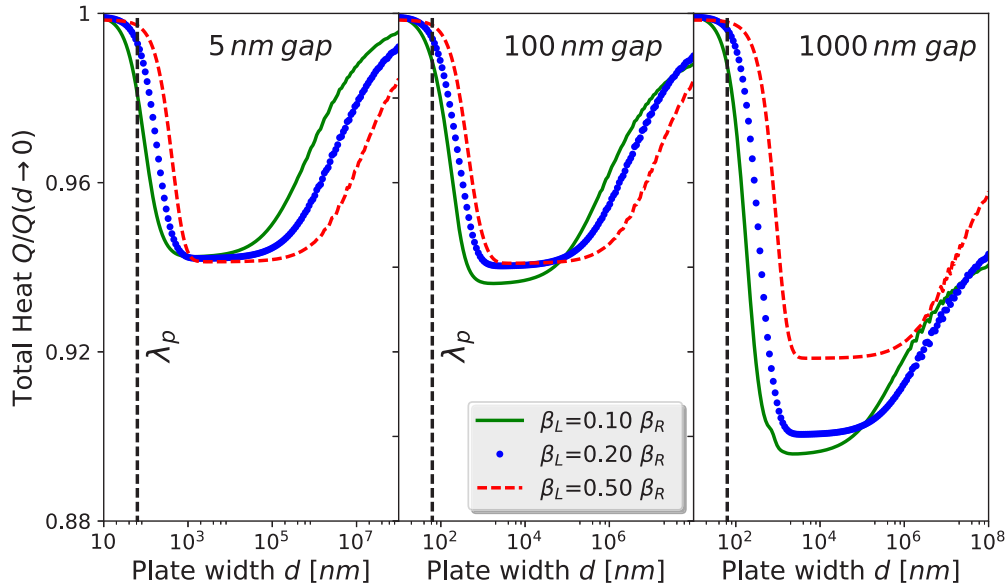


FIG. 5. Normalized total heat with respect to the blackbody radiation impinging ($d = 0$) as a function of the width of the plates for a right temperature $T_{\phi,R} = T_{B,R} = 300$ K and different left temperatures $T_{\phi,L} = T_{B,L}$. Parameters are $\gamma_{L,R} = 10^{-3} \text{ nm}^{-1}$, $\omega_{0,i} = 10^{-1} \text{ nm}^{-1}$, and $\omega_{p,i} = 10^{-1} \text{ nm}^{-1}$. The dashed vertical lines correspond to the value of the plasma wavelength $\lambda_{p1} \equiv \frac{2\pi c}{\omega_{p1}} \approx 63 \text{ nm}$ valid for both plates. $a = 100 \text{ nm}$.

T_L, T_R , which is the one given by Stefan's law for heat exchange between two blackbodies [Eq. (A1)]. On the other hand, for $d \rightarrow +\infty$ (corresponding to the right side of Fig. 4), we have that $Q_{\infty}^{LC} \equiv 0$, while Q_{∞}^B gives Landauer-like formula expressed in Eq. (27).

Considering this, we can analyze the normalized total heat flux between the plates resulting from these contributions at different separation distances a , obtaining Fig. 5 for $T_{\phi,L} = T_{B,L} \equiv T_L$ and $T_{\phi,R} = T_{B,R} \equiv T_R$, with $T_L > T_R$. The normalization is with respect to the blackbody flux corresponding to the expressions for $d = 0$.

From the chosen normalization and previous comments about each contribution for $d = 0$ and $d \rightarrow +\infty$, on one hand, we can identify the left value of each curves as the blackbody heat exchange between the walls of the big oven where the configuration of plates will take place; i.e., they correspond to $Q_{\infty}^{LC}(d = 0)$ for the different temperature differences and they are equal to 1 due to the chosen normalization. As this value is independent of the separation a , it is appropriate to take this criterion for normalizing the total heat in Fig. 5. However, it is worth noting that for each temperature difference, the absolute values of the total heat even at $d = 0$ are different. On the other hand, the right value of the curves correspond to $Q_{\infty}^B(d \rightarrow +\infty)$. The graph then can be interpreted as the competition between both contributions for different values of the thickness d . It is worth noting that this competition gives rise to a minimum of the total heat transfer for a given thickness in the scale of the separation of the plates. Physically, the appearance of the minimum is related to the fact that the plates emitting radiation also act as a shield of the outside radiation coming from the walls of the oven. This behavior is observed when the thickness of the plates d is larger than the plasma wavelength ($\lambda_{p1} \equiv \frac{2\pi c}{\omega_{p1}}$) for the material forming the plates, which in our case corresponds to 63 nm. Then, the net result between how much radiation coming from the walls

is screened by the plates and how much is emitted by them gives the total heat transfer at each thickness d . Thus, for small values of the thickness (with respect to the separation a), we observe that the plates screen more than they emit in the gap, giving a decrease in the heat flux. As the plates get thicker, the screening is increased (decreasing in the gap the amount of radiation coming from the walls of the oven) but also the radiation emitted by the plates to the gap is enhanced. For a given thickness d , the radiation emitted overcomes the screening and the net heat transfer between the plates stops decreasing and begins to increase until the asymptotic value for $d \rightarrow +\infty$, defined only by the radiation emitted by the plates. The scale at which the value of the heat differs in less than 5% is when the thickness is around 10^7 nm , but it gets longer as the separation a increases.

Moreover, although the attenuation of the heat flux with respect to the infinite-thickness ($d \rightarrow +\infty$) value is of the order of 5–6% in every case, with respect to the blackbody flux (when $d = 0$) the percentage of attenuation varies. In fact, for a given separation, it becomes larger as soon as the temperature difference increases. At the same time, the location minimum moves to smaller orders of magnitude as the temperature difference is larger. Then, the percentage of attenuation and the location of the minimum can be tuned by increasing the temperature difference, but only in a simultaneous way.

In Fig. 5, we also see how the total heat flux over the blackbody flux and the mentioned effects depend with the separation a . It can be seen that the attenuation could be increased by enlarging the separation between the plates, and the order of magnitude of thickness to achieve the attenuation becomes smaller too. This responds to the fact that for larger distances, the heat flux between plates provoked by the baths is lower since it involves less evanescent modes when increasing the separation. This is why for a distances of 5nm we observe

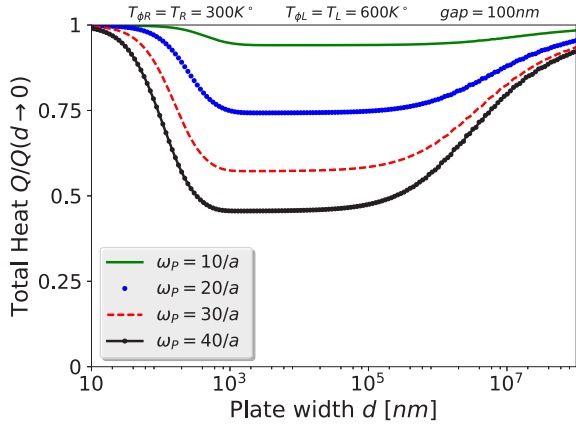


FIG. 6. Normalized total heat with respect to the blackbody radiation impinging ($d = 0$) as a function of the width of the plates for different values of plasma frequencies ω_{p1} . The temperatures are $T_{\phi,R} = T_{B,R} = 300$ K and $T_{\phi,L} = T_{B,L} = 600$ K. Parameters are $\gamma_{L,R} = 10^{-1}/a$, $\omega_{0,i} = 10/a$, and $a = 100$ nm.

that the attenuation is weaker, due to near-field enhancement of heat exchange between the plates.

Nevertheless, increasing both the difference of temperatures or the plates' separation a is not efficient since it demands large thermal gradients or large separations for reaching only a 10% shielding that are not desired for MEMS and NEMS devices. However, we can enhance the shielding (i.e., decrease the heat transfer) by changing the material properties. In Fig. 6, we can see the total normalized heat flux for a given difference of temperatures, a given separation distance, and several values of the plasma frequency ω_{p1} .

Increasing the plasma frequency ω_{p1} implies decreasing the plasma wavelength λ_{p1} , which means that the reflective properties of the plates are improved. Thus, the shielding of the flux related to the initial conditions' contribution is enhanced, decreasing the contribution more rapidly as a function of the thickness d , while the flux associated to the radiated field by each plate does not change to compensate these decays for small thicknesses. As a result, the minimum of the heat flux corresponds to lower percentages of the flux for $d = 0$, reaching almost 60% of attenuation when the plasma frequency is increased by four times.

In terms of materials, we can infer that for dielectrics and metals as gold this attenuation effect may not be significant, while for metals like aluminium or platinum (that have a high-energy plasma frequency value), this effect could not be neglected. In fact, this allows the possibility of measuring and tuning the effect for including it in relevant technological improvements as MEMS and NEMS. Indeed, as the minimum value holds approximately constant in the interval of thicknesses 10^3 – 10^5 nm, having a $1 \mu\text{m}$ of precision on the value of the thickness of the plates is enough to experimentally perceive the attenuation effect when the mentioned metals are employed.

Moreover, considering that the values of the total heat transfer at $d = 0$ and $d \rightarrow +\infty$ are defined by Q_{∞}^{IC} and Q_{∞}^{B} respectively, it is interesting to study the situation where both quantities have opposite signs, which can be achieved by

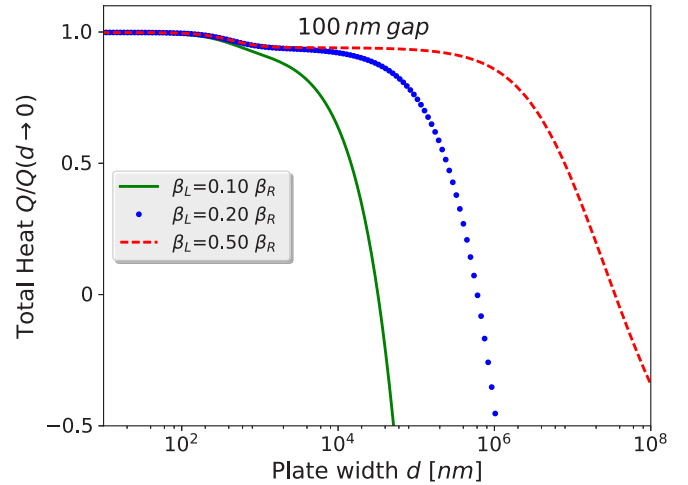


FIG. 7. Normalized total heat with respect to the blackbody radiation impinging ($d = 0$) as a function of the width of the plates for crossed temperatures: $T_{\phi,L} = T_{B,L} = 300$ K and different right temperatures $T_{\phi,R} = T_{B,R}$. Parameters are $\gamma_{L,R} = 10^{-1}/a$, $\omega_{0,i} = 10/a$, and $\omega_{p1,i} = 10/a$, $a = 100$ nm.

setting $T_{\phi,L} > T_{\phi,R}$ and $T_{B,L} < T_{B,R}$. For instance, by taking $T_{\phi,L} = T_{B,R}$ and $T_{\phi,R} = T_{B,L}$, we obtain Fig. 7.

Considering the independence of the values at $d = 0$ and $d \rightarrow +\infty$ and setting it with opposite signs, we showed that there is a thickness for which the heat transfer between the plates (the flux through the gap) is zero. Physically this can be understood because as a cancellation between the screened heat transfer due to the walls of the oven and the heat transfer resulting from the radiation emitted by the plates. This leads to the possibility of thermal shielding inside the gap where no net heat flows from one plate to the other. For the differences on temperature considered, the thickness at which the total heat is zero is between 10^4 and 10^8 nm. This shows that the value can be modified and tuned, for example, by increasing the temperature difference, as can be seen. It is worth noting that varying the separation a does not affect substantially the value of the thickness at which we obtain a zero flux.

VI. CONCLUSIONS

In this work, we have studied different physical aspects of dispersion phenomena in a nonequilibrium scenario, including Casimir force and heat flux. We considered a configuration of two plates of finite width $d_{L,R}$ formed by materials described from a first-principles model, allowing the natural introduction of dissipation, noise, and temperature in the calculations. Using the formalism developed in Ref. [24], we calculate the expectation value of the energy-momentum tensor operator in the steady state as a sum of two contributions, one associated to the initial conditions of the field and the other one associated to the baths in each point of the material plates. This splitting is ensured by the fact that the baths are characterized by thermal states of temperatures $\beta_{B,L}, \beta_{B,R}$ respectively for each plate. For the case of the field, we considered an intrinsic nonequilibrium state, where the modes traveling from left to right ($k > 0$) are at a temperature $\beta_{\phi,L}$, while the modes traveling from right to left ($k < 0$) are at a temperature $\beta_{\phi,R}$. The choice

of this initial state for the field turns out to be crucial at the regularization prescription in order to obtain the nonequilibrium generalization of Lifshitz's formula (force between half-spaces) from the finite-width expressions. Moreover, the correct prescription to calculate the force is the one defined from the subtraction between the radiation pressure between the plates (calculated as a sum of two contributions) and the radiation pressure given without the plates in the appropriate field state, in this case, the intrinsic nonequilibrium. This is the generalization of the well-known Casimir's prescription for the case of nonequilibrium. Here, we point out that the procedure to calculate the force from the difference of the radiation pressures at each side of a given plate gives an incorrect result for the force, which is not symmetric under the exchange of the plates by doing $L \leftrightarrow R$. Then, we give full expressions for both the Casimir force and the heat flux between the plates of widths d_L, d_R .

For the case of the Casimir force, we reproduce particular situations as the expression for dissipationless materials and null widths ($d = 0$). Also, we give insights to obtain the equilibrium Lifshitz formula (for half-spaces), but also its generalization for the nonequilibrium case (taking $d_{L,R} \rightarrow +\infty$), which strongly depends on the intrinsic nonequilibrium state considered for the field. On the other hand, from the numerical analysis, we show that the scale of convergence in the thickness d is of order of the separation a in a configuration of two plates of same dielectric material and width. We can say that the infinite-thickness value for the force is effectively achieved when the width of the plates is of order of the separation between them. Moreover, we showed that the force decreases with the thermal imbalance, with the maximum given by the equilibrium value. We associate this to the fact that in a nonequilibrium scenario, there is an additional momentum transfer between the plates that tends to decrease the value of the net force between them.

For the case of the heat flux between the plates, we also give general expressions but without requiring any regularization since the heat flux is a subtraction between radiations from the very beginning. Regarding the contributions, on one hand, the initial conditions' contribution to the heat flux measures the asymmetry between the blackbody radiations reaching the configuration from each side, which reproduce Stefan's law for blackbody heat exchange when taking $d = 0$. On the other hand, bath contributions are basically the difference between the radiations emitted by each plate, which we show cancel out for the case of null widths ($d = 0$).

It is worth noting that in the general case, we prove that the total heat flux between the plates is not given by a Landauer-like formula. However, the expression for the total heat flux between the plates can be written in terms of differences between the boson occupation numbers at each temperature. In other words, for the general case the total heat flux does not have the form of Landauer unless there are only two different values of temperature in the problem, although it can be expressed as a sum of Landauer-like terms. Moreover, even considering the vacuum state (characterized by zero temperature and number of photons) as the initial state for the field, the heat flux for finite-width plates does not have the Landauer form. Nevertheless, there are some particular cases where the heat flux reduces to Landauer formulas. For example,

we show that for identical plates (same material and width), both contributions result as Landauer formulas separately. If the temperature in one of the contributions agrees with the temperature in the other one, the total heat flux can be written in Landauer form (regardless of the value of the thickness). Also, we show that a Landauer formula is obtained in the case of infinite-thickness for the plates ($d_{L,R} \rightarrow +\infty$), where the initial conditions' contribution goes to zero while the baths' contribution takes Landauer form even for plates of different materials.

In the numerics, for the same scenario analyzed for the force, we first showed that the scale of convergence in thickness of each contribution is several orders of magnitude greater than the case for the force; i.e., the thickness has to be around 10^6 times the separation. For the total heat flux, on the other hand, we found two interesting behaviors as a result of the combination of both contributions.

For the case of considering $T_{\phi,L} = T_{B,L} = T_L \neq T_R = T_{\phi,R} = T_{B,R}$, we showed the formation of a minimum in the heat flux between the plate due to the opposite behaviors of each contribution. We showed that the location of this minimum can be tuned by varying the difference between temperatures $T_{L,R}$. Moreover, the minimum implies that for thicknesses of the order of the plasma wavelength of the material λ_{pI} , there is a shielding of the blackbody radiation impinging on the configuration, while the radiation emitted by the plates becomes important for large thicknesses. The relative percentage with respect to the asymptotic value at $d \rightarrow +\infty$ is on the order of 5–6%, while the blackbody radiation impinging ($d = 0$) depends on the thermal difference and plate separation, giving a chance to have a variable relative percentage but that is not significant. Nevertheless, taking advantage of the fact that λ_{pI} decreases for better reflective materials (higher plasma frequency ω_{pI}), the percentage of attenuation corresponding to the minimum can be tuned by changing the plasma frequency. This responds to the fact that better reflectivity properties result in a better shielding of the initial conditions' contribution while the radiation provided by the plates is not enough to compensate for this effect at small thicknesses, increasing the attenuation to almost 60% when the plasma frequency is four times the typical value for dielectrics. This means that a strong attenuation effect could be attainable with typical metals as aluminium and platinum, being of crucial importance for MEMS and NEMS devices. In other words, we think that our results are important in nanotechnological applications.

Considering the existence of this minimum and regardless of the material considered, we pointed out another interesting issue when considering $T_{\phi,L} = T_{B,R} \neq T_{\phi,R} = T_{B,L}$. We showed that a null heat flux can be achieved for a given thickness. This is explained by the fact that there is a cancellation of the contributions to the heat flux in the gap between the plates. The thickness for which the heat flux vanishes can be tuned by the thermal difference too. This configure a situation of thermal shielding in the gap.

As a final comment, it should be noted that these results can be easily extended to the three-dimensional scalar field, where two kinds of modes enter, the evanescent and the propagating. On the other hand, addressing the extension for the EM case could be in principle a nontrivial issue but is in any case achievable. It is clear that the main complication will be related

to the difficulties associated to quantizing the EM field, which forces us to deal with its gauge invariance and vectorial nature at a quantum framework. However, the conclusions obtained here for the scalar case will remain broadly valid for the EM field. Finally, we left as pending work the possibility of extending this analysis to include different materials and thicknesses, and also changing the temperature differences independently for each contribution.

ACKNOWLEDGMENTS

We would like to thank Ricardo S. Decca for useful comments and discussions on the experimental aspects that are associated to the present work. The work of A.E.R.L. is supported by the Austrian Federal Ministry of Science, Research, and Economy (BMFWF). The work of P.M.P. and F.C.L. is supported by University of Buenos Aires (UBA), CONICET, and ANPCyT.

APPENDIX A: INTRINSIC NONEQUILIBRIUM INITIAL STATE OF THE FIELD

This appendix is devoted to commenting on some of the properties of the mentioned “intrinsic nonequilibrium state” for the initial state of the field. Defined by the expectation values given in Eq. (12), the state basically represents the net radiation flux given in a big oven with its vertical walls at different temperatures $\beta_{\phi,L}$ and $\beta_{\phi,R}$ respectively.

Considering that the annihilation and creation operators for the initial conditions’ contribution $[\hat{a}_k(-\infty), \hat{a}_k^\dagger(-\infty)]$ are the ones of the free field, we can calculate the expectation value of the Poynting vector without the presence of the plates (i.e., free space) for the intrinsic nonequilibrium state. As in this case it is also valid that $\langle \hat{S}_x^{\text{Free}} \rangle_\phi = -\langle \hat{T}_{x0}^{\text{Free}} \rangle_\phi$ and having the field operator given by an expression of the form of Eq. (7) but with the field modes Φ replaced by plane waves $e^{\pm ikx}$ then, by using Eq. (12), we find

$$\begin{aligned} \langle \hat{S}_x^{\text{Free}} \rangle_\phi &= \int_0^{+\infty} dk k \left[\coth\left(\frac{\beta_{\phi,L} k}{2}\right) - \coth\left(\frac{\beta_{\phi,R} k}{2}\right) \right] \\ &= 2 \int_0^{+\infty} dk k [N_{\phi,L}(k) - N_{\phi,R}(k)]. \end{aligned} \quad (\text{A1})$$

Both integrals are easily done as in Ref. [36], giving

$$\langle \hat{S}_x^{\text{Free}} \rangle_\phi = \frac{\pi^2}{3} \left(\frac{1}{\beta_{\phi,L}^2} - \frac{1}{\beta_{\phi,R}^2} \right) = \frac{\pi^2}{3} (T_{\phi,L}^2 - T_{\phi,R}^2), \quad (\text{A2})$$

which have the thermal dependence of the (1+1)-dimensional version of Stefan’s law for the heat exchange through blackbody radiation between two bodies at temperatures $T_{\phi,L}, T_{\phi,R}$. This is the crucial point that allows us to interpret the state defined by Eq. (12) as a nonequilibrium state since it gives a heat flux even in free space. Moreover, since the radiation is blackbody-like, which is far-field radiation, we can think that all the space is inside a big oven with its walls at $x = \pm\infty$ held at different temperatures $T_{\phi,L}, T_{\phi,R}$, causing net heat transfer by radiation going from the hottest side to the other one. In other

words, the intrinsic nonequilibrium state represents the state of the field when there are distant sources in both sides emitting radiation at given different temperatures. It is clear that when $T_{\phi,L} = T_{\phi,R}$, the Poynting vector for free space vanishes.

On the other hand, the energy density for this state is given by

$$\begin{aligned} \langle \hat{T}_{00}^{\text{Free}} \rangle_\phi &= \langle \hat{T}_{xx}^{\text{Free}} \rangle_\phi \\ &= \int_0^{+\infty} dk k \left[\coth\left(\frac{\beta_{\phi,L} k}{2}\right) + \coth\left(\frac{\beta_{\phi,R} k}{2}\right) \right], \end{aligned} \quad (\text{A3})$$

which is the typical expression for the energy density for a thermal state in free space, fully recognizable when setting $T_{\phi,L} = T_{\phi,R}$.

APPENDIX B: COEFFICIENTS

This appendix is devoted to give the expressions of the coefficients that appear in the contributions to the Casimir force and the heat between the plates. For the given configuration of finite-width plates ($d_{L,R}$), the boundary conditions on the modes were continuity of the mode and its spatial derivative at the interfaces between the material slabs and the surrounding vacuum (see Ref. [24] and the references therein). The coefficients then follow

$$T_s = \frac{t_R t_L e^{s(d_L+d_R)}}{1 - r_L r_R e^{-2sa}}, \quad C_s^> = e^{-s d_R} \frac{T_s}{t_R}, \quad D_s^> = e^{-s(a+d_R)} \frac{r_R}{t_R} T_s, \quad (\text{B1})$$

$$\begin{aligned} E_s^> &= \frac{(n_R + 1)}{2n_R} e^{s(n_R-1)(\frac{a}{2}+d_R)} T_s, \\ F_s^> &= \frac{(n_R - 1)}{2n_R} e^{-s(n_R+1)(\frac{a}{2}+d_R)} T_s, \end{aligned} \quad (\text{B2})$$

where we have given the coefficients in terms of the transmission coefficients of the two plates configuration $T_s^>$. Moreover, $r_{L,R}$ and $t_{L,R}$ are the reflection and transmission coefficients for the left and right plates respectively:

$$r_i = \frac{r_{n_i}(1 - e^{-2sn_i d_i})}{(1 - r_{n_i}^2 e^{-2sn_i d_i})}, \quad t_i = \frac{4n_i}{(n_i + 1)^2} \frac{e^{-sn_i d_i}}{(1 - r_{n_i}^2 e^{-2sn_i d_i})}, \quad (\text{B3})$$

with $r_{n_i} = \frac{1-n_i}{1+n_i}$, the reflection coefficient of a surface of refractive index n_i .

It should be noted that the $<$ coefficients are obtained from the given ones by the interchange of L and R in the expressions. Considering this, it turns out that $T_s^> = T_s^<$, which is why the superscript for this coefficient was omitted before.

APPENDIX C: INFINITE-THICKNESS EXPRESSIONS FOR THE FORCE

This appendix is devoted for the limit expressions that are obtained for the infinite-thickness case. This scenario will be

obtained from two approaches. On one hand, by taking the limit $d_{L,R} \rightarrow +\infty$ in Eqs. (16) and (17), as was similarly done in Ref. [24] for the case when $\beta_{\phi,L} = \beta_{\phi,R} \equiv \beta_{\phi}$. On the other hand, we also show that the same result can be obtained from the half-space scenario from the very beginning with the present formalism.

1. Infinite thickness as a limit of the finite width scenario

To successfully take the limit of infinite width on the contributions to the total force, we are going to consider each of them separately. First of all, it is clear that the regularization term $\langle \widehat{T}_{xx}^{\text{Free}} \rangle_{\phi}$ does not depend on the thickness d so the term remains in the limit.

On the other hand, for the initial conditions' contribution it is enough to consider that for $d_{L,R} \rightarrow +\infty$, we have that $r_i \rightarrow r_{n_i}$ while $t_i \rightarrow 0$. Therefore, this allows us to say that $\langle \widehat{T}_{xx}^{\text{IC},\infty} \rangle_{\phi}^{\text{Int}} \rightarrow 0$, regardless of the state considered.

For the bath contribution, we have to take into account more subtle points when taking the limit in some combinations of factors. Considering Eq. (B3), while $t_i \rightarrow 0$, we also have that $|t_i|^2 e^{2\omega \text{Im}(n_i)d_i} \rightarrow \frac{16|n_i|^2}{|n_i+1|^4}$. Therefore, considering the definition for the different coefficients, given in Eq. (B1), and that $1 - |r_{n_i}|^2 = \frac{2\text{Re}(n_i)}{|n_i+1|^2}$, we can write for the factor accompanying $\coth\left(\frac{\beta_{B,L}\omega}{2}\right)$ in Eq. (17):

$$\begin{aligned} & \frac{\text{Re}(n_L)}{2|t_R|^2} \{ |E_{-i\omega}^<|^2 e^{-\omega \text{Im}(n_L)a} [1 - e^{-2\omega \text{Im}(n_L)d_L}] \\ & + |F_{-i\omega}^<|^2 e^{\omega \text{Im}(n_L)a} [e^{2\omega \text{Im}(n_L)d_L} - 1] \\ & + 2 \frac{\text{Im}(n_L)}{\text{Re}(n_L)} \text{Im}[E_{-i\omega}^{<*} F_{-i\omega}^< e^{-i\omega \text{Re}(n_L)a} (1 - e^{-i2\omega \text{Re}(n_L)d_L})] \} \\ & \rightarrow \frac{(1 - |r_{n_L}|^2)}{|1 - r_{n_L} r_{n_R} e^{i2\omega a}|^2}, \end{aligned} \quad (\text{C1})$$

and the same happens for the factor accompanying $\coth\left(\frac{\beta_{B,R}\omega}{2}\right)$, but interchanging L and R.

Therefore, for the contribution of the baths, we have

$$\begin{aligned} & \langle \widehat{T}_{xx}^{\text{B},\infty} \rangle_{\text{B}}^{\text{Int}} [a, d_{L,R} \rightarrow +\infty, \beta_{B,L}, \beta_{B,R}] \\ & = \int_0^{+\infty} d\omega \omega \left[\coth\left(\frac{\beta_{B,L}\omega}{2}\right) \frac{[1 - |r_{n_L}|^2][1 + |r_{n_R}|^2]}{|1 - r_{n_L} r_{n_R} e^{i2\omega a}|^2} \right. \\ & \quad \left. + \coth\left(\frac{\beta_{B,R}\omega}{2}\right) \frac{[1 - |r_{n_R}|^2][1 + |r_{n_L}|^2]}{|1 - r_{n_L} r_{n_R} e^{i2\omega a}|^2} \right]. \end{aligned} \quad (\text{C2})$$

Finally, considering this last expression and subtracting it with the regularization term after setting $\beta_{\phi,L} = \beta_{B,L} \equiv \beta_L$ and $\beta_{\phi,R} = \beta_{B,R} \equiv \beta_R$, we obtain the force between two half-spaces at different temperatures, given by Eq. (23).

After setting thermal equilibrium between the baths and the field ($\beta_{B,L} = \beta_{B,R} = \beta_{\phi,L} = \beta_{\phi,R} \equiv \beta$), the total force reads

$$\begin{aligned} & F_C[a, d_{L,R} \rightarrow +\infty, \beta, \beta, \beta, \beta] \\ & = - \int_{-\infty}^{+\infty} dk k \coth\left(\frac{\beta k}{2}\right) \text{Re} \left[\frac{r_{n_L}(-ik)r_{n_R}(-ik)e^{i2ka}}{1 - r_{n_L}(-ik)r_{n_R}(-ik)e^{i2ka}} \right], \end{aligned} \quad (\text{C3})$$

which is Lifshitz's formula.

2. Infinite-thickness scenario

The expression for the Casimir force between half-spaces at different temperatures and given distance a can be also obtained by considering a half-spaces scenario from the very beginning and applying the same approach developed in Ref. [24].

It is shown that if in the considered scenario there are no infinite-size regions of vacuum or dissipationless material, then the steady situation is defined by the baths' contribution only (there is no initial conditions' contribution in these cases).

Therefore, for the half-spaces scenario from the very beginning, the only contribution to the energy-momentum tensor will be that of the baths.

As in the finite-width case, the contribution of the baths to the field operator will be written in terms of the Green's function of the given problem. Therefore, the expectation value of the components of the energy-momentum tensor can be calculated from Eq. (14). The information about the configuration is clearly enclosed in the Green's function for the considered scenario that can be calculated as in the method commented in Ref. [24].

In the half-spaces scenario, for $-\frac{a}{2} < x < \frac{a}{2}$ and $x' < -\frac{a}{2}$, the Green's function reads

$$\overline{\mathfrak{G}}_{\text{Ret}}(x, x', \omega) = \frac{1}{2i\omega n_L} (A_{-i\omega}^> e^{i\omega x} + B_{-i\omega}^> e^{-i\omega x}) e^{-i\omega n_L x'}, \quad (\text{C4})$$

where the coefficients is given by

$$\begin{aligned} A_s^> & = \frac{2n_L}{(n_L + 1)} \frac{e^{s(n_L-1)\frac{a}{2}}}{(1 - r_{n_R} r_{n_L} e^{-2sa})}, \\ B_s^> & = -\frac{2n_L}{(n_L + 1)} r_{n_R} \frac{e^{s(n_L-3)\frac{a}{2}}}{(1 - r_{n_R} r_{n_L} e^{-2sa})}. \end{aligned} \quad (\text{C5})$$

On the other hand, for $-\frac{a}{2} < x < \frac{a}{2}$ and $\frac{a}{2} < x'$, we have the same expression for $\overline{\mathfrak{G}}_{\text{Ret}}$ but exchanging L with R.

With all these considerations, it can be shown that $\langle \widehat{T}_{xx}^{\text{B},\infty} \rangle_{\text{B}}$ results equal to Eq. (C2). Therefore, to obtain the Casimir force we have to regularize the expression by subtracting the pressure without plates, which is given by Eq. (A3). Finally, it is clear that at the end we obtain the same expression for the nonequilibrium Casimir-Lifshitz force that we obtained from the infinite-thickness limit of the finite width scenario [Eq. (23)].

[1] P. W. Milonni, *The Quantum Vacuum: An Introduction to Quantum Electrodynamics* (Academic Press, San Diego, CA, 1994).

[2] H.-P. Breuer and F. Petruccione, *The Theory of Open Quantum Systems* (Oxford University Press, New York, 2002).

- [3] F. Capasso, J. N. Munday, D. Iannuzzi, and H. B. Chan, *IEEE J. Sel. Top. Quant.* **13**, 400 (2007).
- [4] M. Bordag, U. Mohideen, and V. M. Mostepanenko, *Phys. Rep.* **353**, 1 (2001).
- [5] M. Levin, A. P. McCauley, A. W. Rodriguez, M. T. H. Reid, and S. G. Johnson, *Phys. Rev. Lett.* **105**, 090403 (2010).
- [6] A. W. Rodriguez, F. Capasso, and S. G. Johnson, *Nat. Photon.* **5**, 211 (2011).
- [7] H. Gies, K. Langfeld, and L. Moyaerts, *J. High Energy Phys.* **06** (2003) 018.
- [8] D. A. R. Dalvit, F. C. Lombardo, F. D. Mazzitelli, and R. Onofrio, *Europhys. Letts.* **67**, 517 (2004).
- [9] F. D. Mazzitelli, D. A. R. Dalvit, and F. C. Lombardo, *New J. Phys.* **8**, 240 (2006); D. A. R. Dalvit, F. C. Lombardo, F. D. Mazzitelli, and R. Onofrio, *Phys. Rev. A* **74**, 020101 (2006); Q. Wei, D. A. R. Dalvit, F. C. Lombardo, F. D. Mazzitelli, and R. Onofrio, *ibid.* **81**, 052115 (2010); F. C. Lombardo, F. D. Mazzitelli, and P. I. Villar, *Phys. Rev. D* **78**, 085009 (2008).
- [10] C. D. Fosco, F. C. Lombardo, and F. D. Mazzitelli, *Phys. Rev. D* **84**, 105031 (2011).
- [11] M. Kardar and R. Golestanian, *Rev. Mod. Phys.* **71**, 1233 (1999).
- [12] S. K. Lamoreaux, *Rep. Prog. Phys.* **68**, 201 (2005).
- [13] A. I. Volokitin and B. N. J. Persson, *Rev. Mod. Phys.* **79**, 1291 (2007).
- [14] G. L. Klimchitskaya, U. Mohideen, and V. M. Mostepanenko, *Rev. Mod. Phys.* **81**, 1827 (2009).
- [15] F. C. Lombardo, F. D. Mazzitelli, P. I. Villar, and D. A. R. Dalvit, *Phys. Rev. A* **82**, 042509 (2010).
- [16] F. Intravaia and A. Lambrecht, *Phys. Rev. Lett.* **94**, 110404 (2005).
- [17] I. Pirozhenko and A. Lambrecht, *Phys. Rev. A* **80**, 042510 (2009).
- [18] Y. Luo, R. Zhao, and J. B. Pendry, *P. Nath. Acad. Sci. USA* **111**, 18422 (2014).
- [19] G. Bimonte, T. Emig, M. Kardar, and M. Krüger, *Annu. Rev. Cond. Matt. Phys.* **8**, 119 (2017).
- [20] M. Bordag, [arXiv:1707.06214](https://arxiv.org/abs/1707.06214) (unpublished).
- [21] E. M. Lifshitz, *Sov. Phys. JETP* **2**, 73 (1956).
- [22] I. E. Dzyaloshinskii, E. M. Lifshitz, and L. P. Pitaevskii, *Physics-Uspeski* **4**, 153 (1961).
- [23] F. C. Lombardo, F. D. Mazzitelli, and A. E. R. López, *Phys. Rev. A* **84**, 052517 (2011).
- [24] A. E. Rubio López, *Phys. Rev. D* **95**, 025009 (2017).
- [25] M. Antezza, L. P. Pitaevskii, S. Stringari, and V. B. Svetovoy, *Phys. Rev. A* **77**, 022901 (2008).
- [26] R. O. Behunin and B.-L. Hu, *Phys. Rev. A* **84**, 012902 (2011).
- [27] F. Intravaia and R. O. Behunin, *Phys. Rev. A* **86**, 062517 (2012).
- [28] M. Kruger, G. Bimonte, T. Emig, and M. Kardar, *Phys. Rev. B* **86**, 115423 (2012).
- [29] P. Ben-Abdallah and K. Joulain, *Phys. Rev. B* **82**, 121419(R) (2010).
- [30] P. Ben-Abdallah, S.-A. Biehs, and K. Joulain, *Phys. Rev. Lett.* **107**, 114301 (2011).
- [31] A. E. Rubio López and F. C. Lombardo, *Eur. Phys. J. C* **75**, 93 (2015).
- [32] F. C. Lombardo, F. D. Mazzitelli, A. E. R. Lopez, and G. J. Turiaci, *Phys. Rev. D* **94**, 025029 (2016).
- [33] R. Messina and M. Antezza, *Phys. Rev. A* **84**, 042102 (2011).
- [34] S. Y. Buhmann, *Dispersion Forces I* (Springer-Verlag, Berlin, 2012).
- [35] J. R. Howell, R. Siegel, and M. P. Mengüç, *Thermal Radiation Heat Transfer* (CRC Press, Taylor & Francis, 2010).
- [36] P. T. Landsberg and A. De Vos, *J. Phys. A: Math. Gen.* **22**, 1073 (1989).
- [37] A. Pérez-Madrid, J. M. Rubí, and L. C. Lapas, *J. Non-Equilibrium Thermodyn.* **35**, 279 (2017).
- [38] T. G. Philbin, *New J. Phys.* **12**, 123008 (2010).
- [39] G. Barton, *J. Stat. Phys.* **165**, 1153 (2016).
- [40] R. Yu, A. Manjavacas, and F. J. García de Abajo, *Nat. Comm.* **8**, 2 (2017).
- [41] D. Polder and M. Van Hove, *Phys. Rev. B* **4**, 3303 (1971).
- [42] P. Ben-Abdallah, K. Joulain, J. Drevillon, and G. Domingues, *J. Appl. Phys.* **106**, 044306 (2009).
- [43] I. Latella, P. Ben-Abdallah, S.-A. Biehs, M. Antezza, and R. Messina, *Phys. Rev. B* **95**, 205404 (2017).